 doi:10.20944/preprints201905.0385.v1

Article

Characterization of Photophysical Properties of D–π–A–π–D Type Diketopyrrolopyrrole Based Molecules for Organic Light-Emitting diodes and Organic Solar Cells

Ruifa Jin [1,2,*], Xiaofei Zhang[1,2] and Wenmin Xiao [1,2]

[1] Affiliation 1 College of Chemistry and Chemical Engineering, Chifeng University, Chifeng 024000, China;, skyinthefifthday@126.com (X. Z), xiaowenmin6868@163.com (W.X)

[2] Affiliation Inner Mongolia Key Laboratory of Photoelectric Functional Materials Chifeng 024000, China; skyinthefifthday@126.com (X. Z), xiaowenmin6868@163.com (W.X)

* Correspondence: Ruifajin@163.com (R.J.); Tel: +86-0476-8300370; Fax: +86-0476-8300370.

Abstract: A series of D–π–A diketopyrrolopyrrole (DPP)-based small molecules have been designed for organic light-emitting diodes (OLEDs) and organic solar cells (OSCs) applications. Appling the PBE0/6-31G(d,p) method, the ground state geometry and relevant electronic properties were investigated. The first excited singlet state geometry and the absorption and fluorescent spectra were simulated at the TD-PBE0/6-31G(d,p) level. The calculated results reveal that the photophysical properties are affected through the introduction of different end groups. Furthermore, the electronic transitions corresponding to absorption and emission exhibit intramolecular charge transfer feature. It was disclosed that the designed molecules act not only as luminescent for OLEDs, but also donor materials in OSCs. Moreover, they also can be used as potential electron transfer materials using for OLEDs and OSCs.

Keywords: diketopyrrolopyrrole (DPP)-based molecules; photophysical properties; Charge transporting property; organic light-emitting diodes (OLEDs); organic solar cells (OSCs).

1. Introduction

Organic semiconductors have attracted considerable interest in recent years due to the advantages over their inorganic counterparts, such as low-cost, lightweight, and flexible electronic devices [1–5]. In particular, small-molecule-based organic semiconductors are expected to open new possibilities for their optoelectronic applications in organic electronic devices including organic light-emitting diodes (OLEDs), organic solar cells (OSCs), and field effect transistors (FETs). Small-molecule-based organic semiconductors exhibit strong absorption and emission, high fluorescence quantum yields, and good charge carrier mobility. Nevertheless, the lower efficiency of OLEDs and OSCs has seriously restricted their commercialization application. The development of new small molecular materials with highly desirable properties remains a major challenge. Therefore, it is critically important to design and synthesize efficient multifunctional materials. These materials can serve as efficient light emitting in OLEDs, donor material for OSCs as well as charge transport materials simultaneously [6,7]. In order to achieve high performance and enhance the power conversion efficiency (PCE) of OSCs, the frontier molecular orbitals (FMOs) energy levels of donors should match to typical acceptors. A deep HOMO (highest occupied molecular orbital) energy provides high open circuit voltage (V_{oc}). A relatively high LUMO (lowest unoccupied molecular orbital) energy ensures efficient charge separation. [8–10] Additionally, lower HOMO–LUMO gap (E_g) and strong absorption are required for harvesting the solar photons effectively. The high charge carrier mobility is also demanded for fast charge-carrier transport to maximize the short circuit current (J_{sc}). Furthermore, another key parameter is the downhill

Preprints (www.preprints.org) | NOT PEER-REVIEWED | Posted: 31 May 2019 doi:10.20944/preprints201905.0385.v1

energetic driving force ($\Delta E_{L\text{-}L}$), which is strongly related to the efficient charge transfer. The $\Delta E_{L\text{-}L}$ can be estimated by the energy difference between the LUMO of donor and acceptor, which should at least amount to 0.3 eV [11,12]. Normally, the fullerene derivatives $PC_{61}BM$ ([6,6]-phenyl-C_{61}-butyric acid methyl ester), bis$PC_{61}BM$, and $PC_{71}BM$ are employed as acceptors in OSCs [13,14]. Nowadays, one of the most efficient strategies for optoelectronic materials is to design and synthesize donor–acceptor molecular systems containing a π-bridged (D–π–A) framework [15–18]. The electronic energy levels, absorption and emission spectra, intermolecular stacking, and film morphology can be tuned effectively through chemical modification of acceptor, donor, and π-bridge fragments [19–21]. Amongst various small molecular materials building blocks, diketopyrrolopyrrole (DPP) derivatives have been attracting much interest owing to their outstanding performance in OSCs, OLEDs, and FETs [22–25]. DPP-containing materials possess promising features such as strong absorption and emission in the visible region, excellent thermal and photo-stability, large Stokes shift, and facile synthetic modification [26–30]. The DPP unit is a widely recognized electron acceptor owing to its strong electron-with-drawing nature [31,32]. In the D–π–A molecular systems containing DPP as core, the introduction of aromatic blocks at the 2,5 position of the DPP core can tune the optical properties via π–π intermolecular interactions. Furthermore, the introduction of various end-capping groups onto the aromatic blocks can further tune the molecular properties. Recently, it has been reported that some multifunctional DPP derivatives exhibit good optical property [33].

In the present work, we designed several D–π–A–π–D structure DPP-based small molecules for OSCs and OLEDs applications. These molecules consist of the electron deficient DPP as the core (acceptor), different planar electron-rich aromatic groups as end groups (donor), and benzene as π-bridge (Scheme 1). By mean of density functional theory (DFT) and time-dependent DFT (TD-DFT) computational approach, the photophysical and charge transfer properties were systematically investigated. The FMOs energies (E_{HOMO} and E_{LUMO}), E_g, $\Delta E_{L\text{-}L}$, reorganization energy (λ), and absorption and fluorescent spectra were predicted.

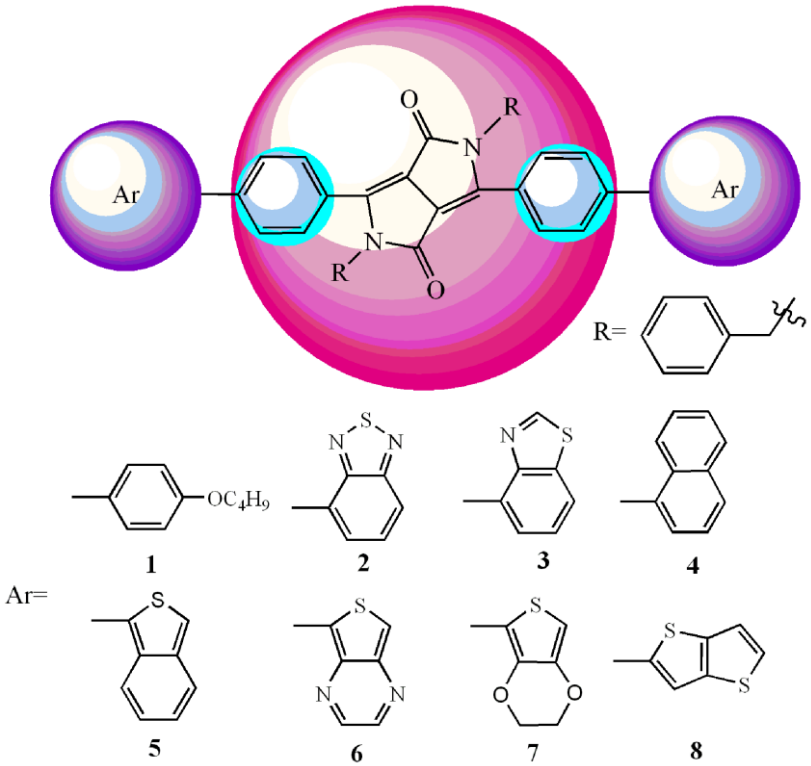

Scheme. 1 Molecular structures of the investigated molecules.

Preprints (www.preprints.org) | NOT PEER-REVIEWED | Posted: 31 May 2019 doi:10.20944/preprints201905.0385.v1

2. Results and Discussion

2.1. Frontier Molecular Orbitals

To gain insight into the influence of the FMO energies on the optical and electronic properties, we have examined the contour plots of HOMOs and LUMOs of the designed molecules, as shown in Figure 1. On the basis of Mulliken population analysis, we also have investigated distribution patterns of FMOs using percentage contributions from DPP, π-bridge (BB), and end groups (EG) moieties by mean of partial density of states (PDOS) (see Table 1). The E_{HOMO}, E_{LUMO}, and E_g of **1**–**8** are plotted in Figure 2. Obviously, the FMOs exhibit π-orbital and strong delocalization features for **1**–**8**, as shown in Figure 2. It is quite obvious that, comparing the contributions of DPP, BB, and EG fragments to the LUMOs with HOMOs, the DPP fragments contributions to LUMOs are smaller than those of to HOMOs for **1**–**4** and **6**–**8**, respectively. On the contrary, the contribution of DPP fragment to LUMO is larger than that of to HOMO for **5**. For the contributions of BB fragments, the contributions to LUMOs are larger than those of to HOMOs for **1**–**5**, **7**, and **8**, respectively. The contribution to LUMO is smaller than that of to HOMO for **6**. For EG fragments, the contributions to LUMOs are larger those of to HOMOs for **2**, **3**, and **6** respectively. However, the contributions to LUMOs are smaller than those of to HOMOs for **1**, **4**, **5**, **7**, and **8**, respectively. Clearly, the vertical $S_0 \rightarrow S_1$ transitions for current system posses the intramolecular charge transfer (ICT) nature. The end groups affect on the distributions of FMOs for D–π–A–π–D molecules.

Table 1. The HOMOs and LUMOs contributions of individual fragments (in %) to the FMOs of **1**–**8** at the PBE0/6-31G(d,p) level.

	HOMOs			LUMOs		
Species	**DPP[a]**	**CB[b]**	**Ar[c]**	**DPP**	**CB**	**Ar**
1	71.0	19.2	9.8	66.1	28.5	5.4
2	75.3	19.0	5.7	33.9	21.1	45.0
3	75.5	19.4	5.1	60.2	30.3	9.5
4	73.1	19.0	7.9	64.3	30.2	5.6
5	47.3	19.7	33.0	54.8	29.8	15.5
6	63.9	21.3	14.9	28.3	21.1	50.6
7	61.2	22.6	16.3	58.2	30.4	11.5
8	61.3	21.0	17.7	56.3	31.1	12.5

[a]DPP: diketopyrrolopyrrole fragment; [b]CB: conjugate bridge moieties. [b]Ar: aromatic groups.

From the results displayed in Figure 2, one can find that the trends of E_{HOMO} and E_{LUMO} are **7** > **1** > **5** > **3** > **6** > **8** > **4** > **2** and **1** > **7** > **3** > **4** > **5** > **8** > **2** > **6**, respectively. It suggests that molecules **2**–**6** and **8** can decrease the E_{HOMO} and E_{LUMO} compared with molecule **1**. However, molecule **7** can increase/decrease the E_{HOMO}/E_{LUMO} compared with that of molecule **1**. Furthermore, the predicted E_g sequence is **4** > **1** > **3** > **7** > **8** > **2** > **5** > **6**. Obviously, molecules **2**, **3**, and **5**–**8** can narrow, whereas molecule **4** can decrease the E_g compared with that of molecule **1**. Consequently, the designed molecules except for **4** may possess longer absorption and fluorescence wavelengths compared with those of molecule **1**. Therefore, one can conclude that the E_{HOMO}, E_{LUMO}, and E_g of the designed D–π–A–π–D molecules can be tuned by different end group groups.

Preprints (www.preprints.org) | NOT PEER-REVIEWED | Posted: 31 May 2019 doi:10.20944/preprints201905.0385.v1

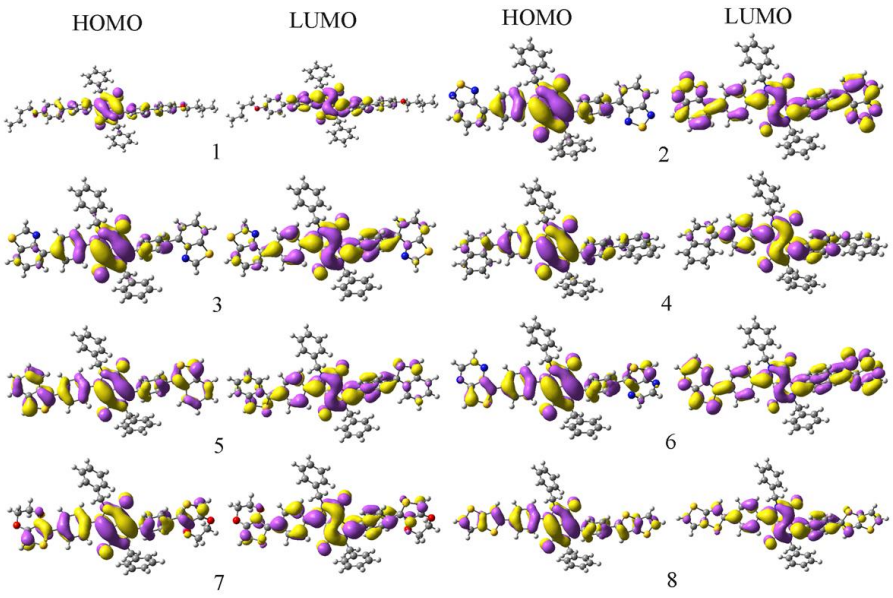

Figure 1. The electronic density contours of the frontier orbital for the studied compounds at the PBE0/6-31G(d,p) level.

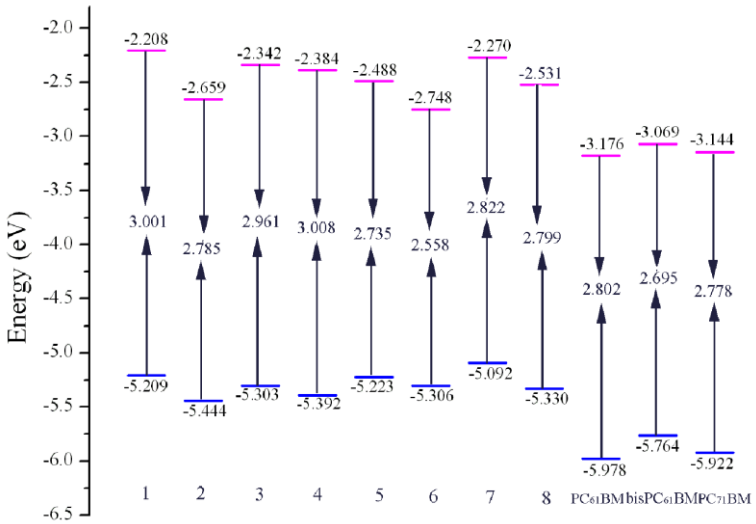

Figure 2. Evaluation of calculated FMO energies for investigated molecules as well as FMO energies for PCBM, bisPCBM, and PC70BM at the PBE0/6-31G(d,p) level.

3.2. Match between Donor and Acceptor Material

It is worth noting that the match between donor and acceptor is crucial for OSCs devices. Namely, donor materials should possess suitable FMOs energy levels. Firstly, with the aim of efficient electron transfer, the E_{LUMO} of donor should be higher than that of acceptor. Additionally, the $\Delta E_{L\text{-}L}$ should be larger than the binding energy (0.2–1.0 eV) [38,39] and should at least attain to 0.3 eV. Secondly, in order to improve the performance of OSCs, donor materials should exhibit higher J_{sc} and V_{oc} and efficient charge transfer. Therefore, the lower E_g are required for ensuring the harvesting sunlight effectively and enhancing the J_{sc}. The large difference between the E_{HOMO} of donor and the E_{LUMO} of acceptor is favorable for enhancing the V_{oc} and efficient exciton dissociation [34–37].

We take $PC_{61}BM$, $bisPC_{61}BM$, and $PC_{71}BM$ as acceptors for current system (see Figure 2). We calculated the $\Delta E_{L\text{-}L}$ of **1**–**8** (see Table 2). As visualized in Figure 2, the E_{LUMO} of **1**–**8** are positioned above that of $PC_{61}BM$, $bisPC_{61}BM$, and $PC_{71}BM$, respectively. When $PC_{61}BM$, $bisPC_{61}BM$, and $PC_{71}BM$ are taken as acceptors, the predicted $\Delta E_{L\text{-}L}$ of **1**–**8** are 0.428–0.968, 0.321–0.861, and 0.396–0.963 eV, respectively. Obviously, they are all exceed 0.3 eV. As a consequence, the electron transfer to acceptors is efficient for these molecules. On the other hand, the E_{HOMO} of the designed molecules are lower 1.916, 2.023, and 1.9481 eV than

Preprints (www.preprints.org) | NOT PEER-REVIEWED | Posted: 31 May 2019 doi:10.20944/preprints201905.0385.v1

the E_{LUMO} of $PC_{61}BM$, $bisPC_{61}BM$, and $PC_{71}BM$, respectively. With the above considerations, the designed molecules possess suitable FMO energies to match those of three typical fullerene acceptors. Therefore, the FMOs of these molecules can be tuned by the planar electron-rich aromatic end groups to match $PC_{61}BM$, $bisPC_{61}BM$, and $PC_{71}BM$ acceptors.

Table 2. The calculated $\Delta E_{L\text{-}L}$ for **1–8** at the PBE0/6-31G(d,p).

Species	$\Delta E_{L\text{-}L}$[a]	$\Delta E_{L\text{-}L}$[b]	$\Delta E_{L\text{-}L}$[c]
1	0.968	0.861	0.936
2	0.517	0.410	0.485
3	0.834	0.727	0.802
4	0.792	0.685	0.760
5	0.688	0.581	0.656
6	0.428	0.321	0.396
7	0.906	0.799	0.874
8	0.645	0.538	0.613

[a] $\Delta E_{L\text{-}L}$ for PCBM as acceptor; [b] $\Delta E_{L\text{-}L}$ for bisPCBM as acceptor; [c] $\Delta E_{L\text{-}L}$ for PC70BM as acceptor.

3.3. Absorption and Fluorescent Properties

Tables 3 and 4 collected the predicted properties of absorption and fluorescence spectra of the designed molecules, respectively. The simulated absorption and fluorescence spectra of **1–8** are shown in Figures 3 and 4. For the absorption spectra, clearly, they are mainly derived from HOMOs → LUMOs transitions with 71% contributions for **1–8**. The longest wavelengths of absorption (λ_{abs}) of molecules **2**, **3**, and **5–8** show bathochromic shifts 43.4, 5.4, 52.1, 93.7, 29, and 36.1 nm, whereas molecule **4** exhibit hypsochromic shift 2.3 nm compared with that of molecule **1**, respectively. At the same time, the λ_{abs} is in the order of **6** > **5** > **2** > **8** > **7** > **3**> **1** > **4**, which is in excellent agreement with the corresponding reverse order of E_g values. Moreover, one can find in that molecules **6–8** has larger *f* value than that of **1**, while the while the corresponding values of *f* values of **2–5** are slightly less than that of **1**, respectively. Generally, larger *f* value corresponds to larger experimental absorption coefficient or stronger fluorescence intensity. It suggests that molecules **2**, **3**, and **5–8** can increase the λ_{abs} values compared with molecule **1**. On the other hand, molecule **4** does not significantly affect the λ_{abs} compared with molecule **1**. Therefore, the designed molecules can be used as donor materials for OSCs applications.

The longest wavelengths of fluorescence (λ_{flu}) of **1–8** mainly originate from the LUMOs → HOMOs excitations, as shown in Table 4. Similar to those absorption spectra, the λ_{flu} of molecules **2**, **3**, and **5–8** show bathochromic shifts 62.3, 6.8, 119.9, 51.5, 22, and 37.9 nm compared with molecule **1**, respectively. On the contrary, molecule **4** exhibit hypsochromic shift 5.3 nm◎ compared with that of **1**. The λ_{flu} value is in the sequence **5** > **2** > **6** > **8** > **7** > **3** > **1** > **4**. Furthermore, the *f* values of **2–5** are slightly less than that of **1** and the corresponding values of molecules **6–8** are larger than that of molecules **1**, respectively. Therefore, the designed molecules have large fluorescent intensity. As a consequence, they can be used as luminescent materials for OLEDs, particularly for **6–8**.

The results displayed in Tables 2 and 3 reveal that the absorption and fluorescence spectra of the designed molecules can be affected significantly by end groups. The designed molecules exhibit larger absorption coefficient and stronger fluorescence intensity. It suggests that these molecules can serve not only as luminescent for OLEDs, but also donor materials in OSCs.

Preprints (www.preprints.org) | NOT PEER-REVIEWED | Posted: 31 May 2019 doi:10.20944/preprints201905.0385.v1

Table 3. Predicted longest wavelength of absorption, corresponding oscillator strength *f*, and main assignment of **1–8** at the TD- PBE0/6-31G(d,p)//PBE0/6-31G(d,p) level.

Species	λ_{abs} (nm)	*f*	Assignment
1	478.2	0.93	HOMO → LUMO (0.71)
2	521.6	0.74	HOMO → LUMO (0.70)
3	483.6	0.90	HOMO → LUMO(0.71)
4	475.9	0.82	HOMO → LUMO(0.71)
5	530.3	1.25	HOMO → LUMO (0.71)
6	571.9	0.96	HOMO → LUMO(0.70)
7	507.2	1.14	HOMO → LUMO(0.71)
8	514.3	1.28	HOMO → LUMO(0.70)
Exp[b]	494		

[a] Experimental data for **1** were taken from Ref. [33].

Table 4. Predicted longest wavelength of fluorescence, corresponding oscillator strength *f*, and main assignment of **1–8** at the TD-PBE0/6-31G(d,p)//TD-PBE0/6-31G(d,p) level.

Species	λ_{flu}	*f*	Assignment
1	565.6	1.08	HOMO ← LUMO (0.71)
2	627.9	0.83	HOMO ← LUMO (0.71)
3	572.4	1.03	HOMO ← LUMO(0.71)
4	560.3	0.95	HOMO ← LUMO(0.71)
5	685.5	1.01	HOMO ← LUMO (0.71)
6	617.1	1.46	HOMO ← LUMO(0.71)
7	587.6	1.23	HOMO ← LUMO(0.71)
8	603.5	1.44	HOMO ← LUMO(0.71)
Exp[1]	562		

[a] Experimental data for **1** were taken from Ref. [33].

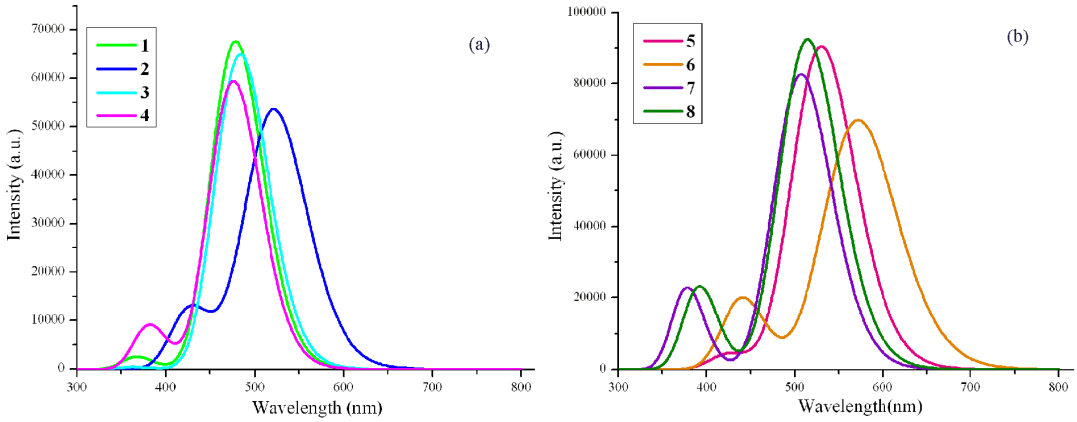

Figure 3. The calculated absorption spectra of the investigated molecules (value of full width at half maximum is 3000 cm^{-1}). (a) Molecules **1–4**; (b) Molecules **5–8**.

Preprints (www.preprints.org) | NOT PEER-REVIEWED | Posted: 31 May 2019 doi:10.20944/preprints201905.0385.v1

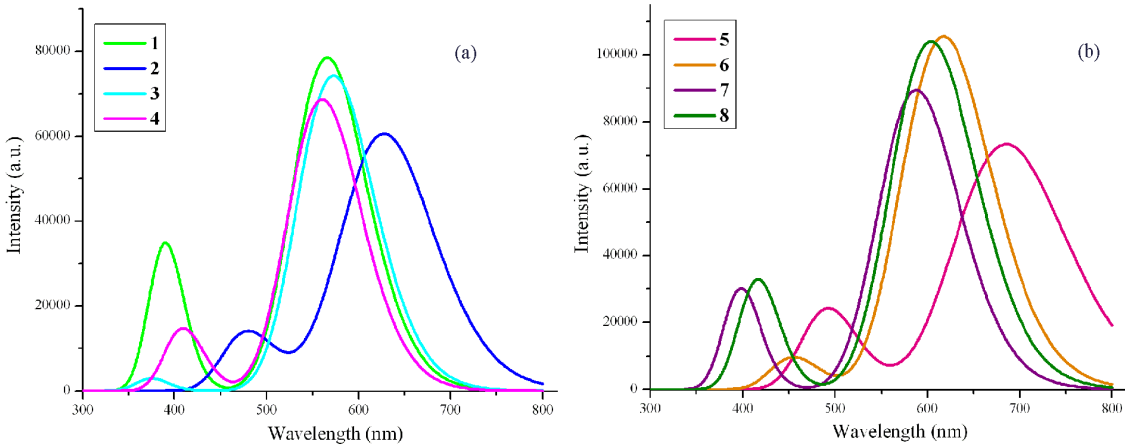

Figure 4. The calculated fluorescence spectra of the investigated molecules (value of full width at half maximum is 3000 cm^{-1}). (a) Molecules **1**–**4**; (b) Molecules **5**–**8**.

3.4. Reorganization Energies and Stabilities

The predicted λ_e and λ_h of **1**–**8** are listed in Table 5. It is quite clear that the λ_h of **1**–**8** are larger than those of the λ_e, respectively. It suggests that rates of electron transfer may higher than rates of hole transfer for **1**–**8**, respectively. Interestingly, molecule **1** possesses the largest both λ_e and λ_h values, indicating that the introduction of different end groups can lower the λ_e and λ_h for the designed molecules. Furthermore, molecules **5** and **6** exhibit the smallest λ_h and λ_e, respectively. From these results, it can be found that the introduction of different end groups is favourable for hole and electron transfer. They may act as electron transport materials in OLEDs and OSCs.

Usually, the stability of materials can be predicted by mean of the η value. As shown in Table 5, the η value of molecule **4** is larger than the value of molecule **1**. However, as expected, molecules **2**, **3** and **5**–**8** possess slightly smaller than that of molecule **1**. Compared with molecule **1**, the stabilities of **2**, **3** and **5**–**8** decrease slightly because of their steric hindrances. It suggests that the end groups have a little effect on the stability of molecules.

Another way to evaluate the stability of material is to analyze the electrostatic surface potentials. Therefore, the electrostatic surface potentials of the designed molecules were calculated and plotted in Figure 5. The high negative charges of 1–8 are resided at the two oxygen atoms of DPP moieties, as visualized in Figure 5. The reason may be the presence lone pairs on oxygen atoms. On the contrary, partial positive charges are on the aromatic end groups. It can be observed that molecules **1**–**8** have the similar positive and negative potential distribution, implying that they possess same magnitude of photostability. Apparently, these results also reveal that the introduction of different end groups has lightly affected on the stability of the molecules.

Table 5. Calculated λ_e, λ_h, and η (all in eV) of **1**–**8** at the PBE0/6-31G(d,p) level.

Species	λ_h	λ_e	η
1	0.401	0.343	2.284
2	0.374	0.240	2.174
3	0.386	0.322	2.277
4	0.364	0.315	2.305
5	0.325	0.260	2.104
6	0.356	0.222	2.017
7	0.392	0.278	2.180
8	0.380	0.263	2.145

Preprints (www.preprints.org) | NOT PEER-REVIEWED | Posted: 31 May 2019 doi:10.20944/preprints201905.0385.v1

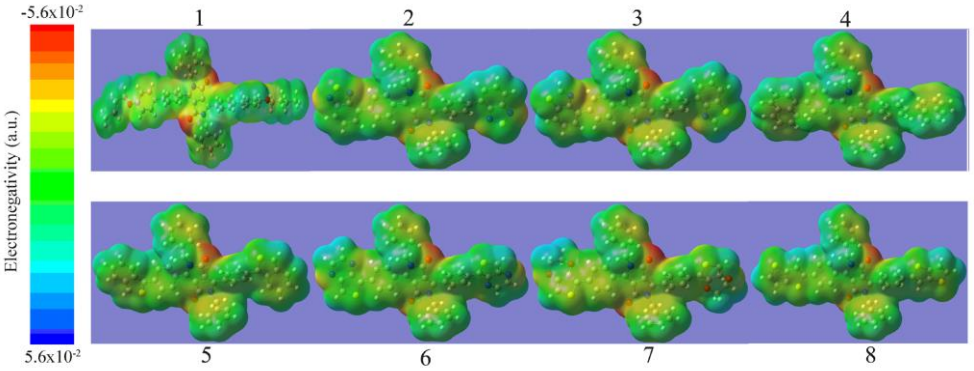

Figure 5. Electrostatic surface potentials for designed molecules. Regions of higher and lower electron density are shown in red and blue, respectively (values in atomic units).

3. Materials and Methods

Computational Methods

All the calculations were carried out using Gaussian 09 suite of programs [40]. The DFT was employed to perform the geometry optimization and frequency calculations of the molecules in ground states (S_0). The frequency analysis characterizes that the optimized structures are true minima. The equilibrium geometries of the molecules in the first excited singlet state (S_1) were optimized by mean of TD-DFT method. On the basis of optimized structures in S_0 and S_1, the absorption and fluorescent spectra were simulated by TD-DFT method, respectively. With the aim to choose reasonable method, differents functionals were taken to optimize the geometry of **1** in S_0 and S_1. These functionals contain such as B3LYP [41], PBE0 [42], CAM-B3LYP [43], M062X [44], MPW1PW91 [45], and ωB97XD [46]. Under the optimized structures in S_0 and S_1, the absorption and fluorescent spectra of molecule **1** were predicted using the TD-DFT method. The λ_{abs} and λ_{flu} are plotted in Figure 6. The tested results reveal that the λ_{abs} and λ_{flu} (478.2 and 565.6 nm) using PBE0 (583 nm) method are well reproduce the experimental results (494 and 562 nm) [33], and the deviations are 15.8 and 3.6 nm, respectively. The Stokes shift is 87.4 nm, which is comparable to the experimental 68 nm. As a consequence, PBE0 method is the best choice to investigate our system. The PBE0 was also used to optimize the acceptors $PC_{61}BM$, $bisPC_{61}BM$, and $PC_{71}BM$. The 6-31G (d,p) basis set was used for all the calculations.

It is commonly known that the reorganization energy (λ) is a key parameter for charge transfer rates [47,48]. The lower electron (λ_e) and hole (λ_h) reorganization energies are beneficial for the higher electron and hole transfer rates, respectively. In this work, we only consider the internal λ owing to ignoring any environmental relaxation and changes. The λ_e and λ_h values were predicted at the PBE0/6-31G(d,p) level on the basis of the single point energy. The λ_e and λ_h can be evaluated by the following equations [49]:

$$\lambda_e = \left(E_0^- - E_-^-\right) + \left(E_-^0 - E_0^0\right) \quad (1)$$

$$\lambda_h = \left(E_0^+ - E_+^+\right) + \left(E_+^0 - E_0^0\right) \quad (2)$$

where $E_0^{\pm}$ is the energy of cation/anion structure based on the optimized neutral structure. Conversely, $E_{\pm}^0$ represent the energy of neutral structure based on optimized cation/anion structure. Similarly, $E_{\pm}^{\pm}$ is the energy of cation/anion structure based on the optimized cation/anion structure, while E_0^0 is the energy of the neutral molecule at ground state.

It is critically important to evaluate the stability of the material in the devices for OSCs and OLEDs. The absolute hardness (η) of materials can be used as useful criterion to investigate the stability of the material. The η values can be predicted using the following equation: [50,51]

Preprints (www.preprints.org) | NOT PEER-REVIEWED | Posted: 31 May 2019 doi:10.20944/preprints201905.0385.v1

$$\eta = \frac{1}{2}\left(\frac{\partial \mu}{\partial N}\right) = \frac{1}{2}\left(\frac{\partial^2 E}{\partial N^2}\right) = \frac{AIP - AEA}{2} \quad (3)$$

Where, μ and N are the chemical potential and total electron number, respectively. *AIP* and *AEA* correspond to the adiabatic ionization potential and adiabatic electron affinity, respectively.
The *AIP* is the energy difference between the cation radical and its neutral species, while the *AEA* represents the energy difference between the neutral and its anion radical molecules. The PBE0/6-31G(d,p) method was applied to calculate the *AIP* and *AEA* of the molecules. The electrostatic surface potentials also can be used to estimate the stability properties of molecules [52–54]. Therefor, we calculated the electrostatic surface potentials of molecules at the PBE0/6-31G(d,p) level.

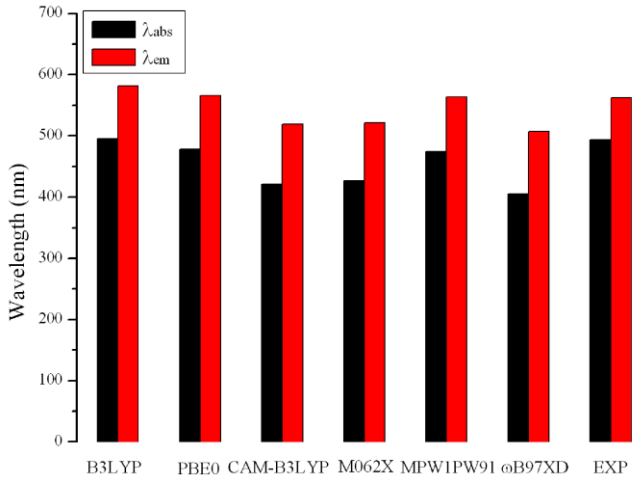

Figure 6. Calculated absorption and fluorescence wavelengths (λ_{abs} and λ_{flu}) of molecule **1** using various functionals, together with the experimental result.

4. Conclusions

Several D–π–A type DPP-based small molecules were designed for OLEDs and OSCs applications. Their photophysical and charge transfer properties were investigated using DFT and TD-DFT computational approaches. The calculated results reveal that the photophysical properties are affected through the introduction of different end groups. Furthermore, the electronic transitions corresponding to absorption and emission exhibit intramolecular charge transfer feature. Additionally, the designed molecules possess suitable FMO energies to match those of three typical fullerene acceptors $PC_{61}BM$, $bisPC_{61}BM$, and $PC_{71}BM$. It was disclosed that the designed molecules act not only as luminescent for OLEDs, but also donor materials in OSCs. Moreover, they also can be used as potential electron transfer materials using for OLEDs and OSCs.

Author Contributions: Ruifa Jin conceived and designed the calculations; Xiaofei Zhang contributed to the performance and analysis of the frontier molecular orbitals and absorption and fluorescent spectra; Wenmin Xiao performed the reorganization energies and transport properties; Xiaofei Zhang helped with results interpretation. Ruifa Jin wrote the paper.

Acknowledgments: Financial supports from the NSFC (No. 21563002) are gratefully acknowledged.

Conflicts of Interest: The authors declare that they have no conflict of interest.

Appendix

OSCs	Organic solar cells
OLEDs	Organic light-emitting diodes
FETs	Field effect transistors

 doi:10.20944/preprints201905.0385.v1

$\Delta E_{L\text{-}L}$	Downhill energetic driving force
DPP	Diketopyrrolopyrrole
ICT	Intramolecular charge transfer
DFT	Density function theory
TD-DFT	Time dependent density function theory
FMOs	Frontier molecular orbital energies
HOMO	Highest occupied molecular orbital
LUMO	Lowest unoccupied molecular orbital

References

1. Grimsdale, A.C.; Chan, K.L.; Martin, R.E.; Jokisz, P.G.; Holmes, A.B. Synthesis of light-emitting conjugated polymers for applications in electroluminescent devices. *Chem. Rev.* **2009**, *109*, 897–1091.
2. Klauk, H. Organic thin-film transistors. *Chem. Soc. Rev.* **2010**, *39*, 2643–2666.
3. Li, X.; Choy, W.; Huo, L.; Xie, F.; Sha, W.; Ding, B.; Guo, X.; Li, Y.; Hou, J.; You, J.; Yang, Y. Dual plasmonic nanostructures for high performance inverted organic solar cells. *Adv. Mater.* **2012**, *24* 3046–3052.
4. Minaev, B.; Baryshnikov, G.; Agren, H. Principles of phosphorescent organic light emitting devices. *Phys. Chem. Chem. Phys.* **2014**, *16*, 1719–1758.
5. Zhu, Y.; Yuan, Z.; Cui, W.; Wu, Z.; Sun, Q.; Wang, S.; Kang, Z.; Sun, B. A cost-effective commercial soluble oxide cluster for highly efficient and stable organic solar cells. *J. Mater. Chem. A* **2014**, *2*, 1436–1442.
6. Han, L.; Wang, C.; Ren, A.; Liu, Y.; Liu, P. Structural and optical properties of triphenylamin-substituted anthracene derivatives. *J. Mol. Sci.* **2013**, *29*, 146–151.
7. Sahu, D.; Tsai, C.H.; Wei, H.Y.; Ho, K.C.; Chang, F.C.; Chu, C.W. Synthesis and applications of novel low bandgap star-burst molecules containing a triphenylamine core and dialkylated diketopyrrolopyrrole arms for organic photovoltaics. *J. Mater. Chem.* **2012**, *22*, 7945–7953.
8. Li, J.; Ong, K. H.; Lim, S. L.; Ng, G. M.; Tan, H. S.; Chen, Z. K. A random copolymer based on dithienothiopheneand diketopyrrolopyrrole units for high performance organic solar cells. *Chem. Commun.* **2011**, *47* 9480–9482.
9. Coughlin, J. E.; Henson, Z. B.; Welch, G. C.; Bazan, G. C. Design and synthesis of molecular donors for solution-processed high-efficiency organic solar cells. *Acc. Chem. Res.* **2014**, *47* 257–270.
10. Huang, Y.; Zhang, M.; Chen, H.; Wu, F.; Cao, Z.; Zhang, L.; Tan, S. Efficient polymer solar cells based on terpolymers with a broad absorption range of 300–900 nm. *J. Mater. Chem. A* **2014**, *2*, 5218–5223.
11. Scharber, M.C.; Wuhlbacher, D.; Koppe, M.; Denk, P.; Waldauf, C.; Heeger, A.J.; Brabec, C.L. Design rules for donors in bulk-heterojunction solar cells-towards 10 % energy-conversion efficiency. *Adv. Mater.* **2006**, *18*, 789–794.
12. Brédas, J.L.; Beljonne, D.; Coropceanu, V.; Cornil, J. Charge-transfer and energy-transfer processes in π-conjugated oligomers and polymers: a molecular picture. *Chem. Rev.* **2004**, *104*, 4971–5004.
13. He, C.; He, Q.G.; Yang, X.D.; Wu, G.L.; Yang, C.H.; Bai, F.L.; Shuai, Z.G.; Wang, L.X.; Li, Y.F. Synthesis and photovoltaic properties of a solution-processable organic molecule containing triphenylamine and DCM moieties. *J. Phys. Chem. C* **2007**, *111*, 8661–8666.
14. Lenes, M.; Wetzelaer, G.A.H.; Kooistra, F.B.; Veenstra, S.C.; Hummelen, J.C.; Blom, P.W.M. Fullerene bisadducts for enhanced open-circuit voltages and efficiencies in polymer solar cells. *Adv. Mater.* **2008**, *20*, 2116–2119.
15. Cheng, H.; Zhao, X.; Shen, Y.; Wang, M.; Wang, L.; Meier, H.; Cao, D. Diketopyrrolopyrrole based D- π-A- π-D type small organic molecules as hole transporting materials for perovskite solar cells. *J. Energy. Chem.* **2018**, *27*, 1175-1182.
16. Zhang, S.; Niu, Q.; Sun, T.; Li, Y.; Li, T.; Liu, H. The synthesis and properties of linear A–π–D–π–A type organic small molecule containing diketopyrrolopyrrole terminal units. *Spectrochim. Acta. A* **2017**, *183*, 172–176.
17. Zhang, S.; Sun, T.; Xu, Z.; Li, T.; Li, Y.; Niu, Q.; Liu, H. Novel biphenylene-diketopyrrolopyrrole-based A-π-D-π–A molecule: Synthesis, optical, electrochemical and electronical properties. *Tetrahedron. Lett.* **2017**, *58*, 2779–2783.
18. Liu, H.; Jia, H.; Wang, L.; Wu, Y.; Zhan, C.; Fu, H.; Yao, J. Intermolecular electron transfer promoted by directional donor–acceptor attractions in self-assembled diketopyrrolopyrrole-thiophenefilms. *Phys. Chem. Chem. Phys.* **2012**, *14*, 14262–14269.
19. Wang, M.; Wang, H.; Yokoyama, T.; Liu, X.; Huang, Y.; Zhang, Y.; Nguyen, T.Q.; Aramaki, S.; Bazan, G.C. High open circuit voltage in regioregular narrow band gap polymer solar cells. *J. Am. Chem. Soc.* **2014**, *136*, 12576–12579.
20. Wang, E.; Mammo, W.; Andersson, M.R. 25th Anniversary article: isoindigo-based polymers and small molecules for bulk heterojunction solar cells and field effect transistors. *Adv. Mater.* **2014**, *26*, 1801–1826.
21. Chen, S.; Xiao, L.; Zhu, X.; Peng, X.; Wong, W.K.; Wong, W.Y. Solution-processed new porphyrin-based small molecules as electron donors for highly efficient organic photovoltaics. *Chem. Commun.* **2015**, *51*, 14439–14442.
22. Lin, Y.; Cheng, P.; Li, Y.; Zhan, X.A. A 3D star-shaped non-fullerene acceptor for solution-processed organic solar cells with a high open-circuit voltage of 1.18 V. *Chem. Commun.* **2012**, *48*, 4773–4775.

23. Bürckstümmer, H.; Weissenstein, A.; Bialas, D.; Würthner, F. Synthesis and characterization of optical and redox properties of bithiophene-functionalized diketopyrrolopyrrole chromophores. *J Org. Chem.* **2011**, *76*, 2426–2432.
24. Chen, H.; Guo, Y.; Yu, G.; Zhao, Y.; Zhang, J.; Gao, D.; Liu, H.; Liu, Y. Highly π-extended copolymers with diketopyrrolopyrrole moieties for high-performance field-effect transistors. *Adv. Mater.* **2012**, *24*, 4618–4622.
25. Ha, J.S.; Kim, K.H.; Choi, D.H. 2,5-Bis(2-octyldodecyl)pyrrolo[3,4-*c*]pyrrole-1,4-(2*H*,5*H*)-dione-based donor-acceptor alternating copolymer bearing 5,5′-di(thiophen-2-yl)-2,2′-biselenophene exhibiting 1.5 $cm^2 \cdot v^{-1} \cdot s^{-1}$ hole mobility in thin-film transistors. *J. Am. Chem. Soc.* **2011**, *133*, 10364–10367.
26. Dhar, J.; Venkatramaiah, N.; Anitha, A.; Patil, S. Photophysical, electrochemical and solid state properties of diketopyrrolopyrrole based molecular materials: importance of the donor group. *J. Mater. Chem. C* **2014**, 2, 3457–3466.
27. Jin, Y.; Xu, Y.; Liu, Y.; Wang, L.; Jiang, H.; Cao, D.R. Synthesis of novel diketopyrrolopyrrole-based luminophores showing crystallization-induced emission enhancement properties. *Dyes. Pigm.* **2011**, *90*, 3110–3118.
28. Shen, X.Y.; Wang, Y.J.; Zhang, H.; Qin, A.; Sun, J.Z.; Tang, B.Z. Conjugates of tetraphenylethene and diketopyrrolopyrrole: tuning the emission properties with phenyl bridges. *Chem. Commun.* **2014**, *50*, 8747–8750.
29. Szabadai, R.S.; Roth-Barton, J.; Ghiggino, K.P.; White, J.M.; Wilson, D.J.D. Solvatochromism in diketopyrrolopyrrole derivatives: experimental and computational studies. *Aust. J. Chem.* **2014**, *67*, 1330–1337.
30. Wang, Y.; Huang, Q.; Liu, Z.; Li, H. A perfluorohexyl containing diketopyrrolopyrrole (DPP) small molecule for high performance ambipolar transistors with balanced hole and electron mobilites. *RSC Adv.* **2014**, *4*, 29509–29513.
31. Roland, T.; Heyer, E.; Liu, L.; Ruff, E.; Ludwigs, S.; Ziessel, R.; Haacke, S. Unsymmetrical donor-acceptor-acceptor-π-donor type benzothiadiazole-based small molecule for a solution processed bulk heterojunction organic solar cell. *ACS Appl. Mater. Interfaces.* **2015**, *7*, 10283–10292.
32. Heyer, E.; Ziessel, R. Panchromatic push-pull dyes of elongated form from triphenylamine, diketopyrrolopyrrole, and tetracyanobutadiene modules. *Synlett.* **2015**, *26*, 2109–2116.
33. Kuwabara, J.; Yamagata, T.; Kanbara, T. Solid-state structure and optical properties of highly fluorescent diketopyrrolopyrrole derivatives synthesized by cross-coupling reaction. *Tetrahedron.* **2010**, *66*, 3736–3741.
34. Li, J.; Ong, K.H.; Lim, S.L.; Ng, G.M.; Tan, H.S.; Chen, Z.K. A random copolymer based on dithienothiophene and diketopyrrolopyrrole units for high performance organic solar cells. *Chem. Commun.* **2011**, *47*, 9480–9482.
35. Coughlin, J.E.; Henson, Z.B.; Welch, G.C.; Bazan, G.C. Design and synthesis of molecular donors for solution-processed high-efficiency organic solar cells. Acc. Chem. Res. 2014, 47, 257–270.
36. Stuart, A.C.; Tumbleston, J.R.; Zhou, H.; Li, W.; Liu, S.; Ade, H.; You, W. Fluorine substituents reduce charge recombination and drive structure and morphology development in polymer solar cells. *J. Am. Chem. Soc.* **2013**;*135*, 1806–1815.
37. Kim, H.; Lee, H.; Seo, D.; Jeong, Y.; Cho, K.; Lee, J.; Lee, Y. Regioregular low bandgap polymer with controlled thieno[3,4-b]thiophene orientation for highefficiency polymer solar cells. *Chem Mater.* **2015**, *27*, 3102–3107.
38. Knupfer, M. Exciton binding energies in organic semiconductors. *Appl. Phys. A* **2003**, *77*, 623–626.
39. Hill, I.G.; Kahn, A.; Soos, Z.G.; Pascal Jr, R.A. Charge-separation energy in films of π-conjugated organic molecules. *Chem. Phys. Lett.* **2000**, *327*, 181–188.
40. M.J. Frisch, G.W. Trucks, H.B. Schlegel, G.E. Scuseria, M.A. Robb, J.R. Cheeseman, G. Scalmani, V. Barone, B. Mennucci, G.A. Petersson, H. Nakatsuji, M. Caricato, X. Li, H.P. Hratchian, A.F. Izmaylov, J. Bloino, G. Zheng, J.L. Sonnenberg, M. Hada, M. Ehara, K. Toyota, R. Fukuda, J. Hasegawa, M. Ishida, T. Nakajima, Y. Honda, O. Kitao, H. Nakai, T. Vreven, J.A. Montgomery, Jr, J.E. Peralta, F. Ogliaro, M. Bearpark, J.J. Heyd, E. Brothers, K.N. Kudin, V.N. Staroverov, T. Keith, R. Kobayashi, J. Normand, K. Raghavachari, A. Rendell, J.C. Burant, S.S. Iyengar, J. Tomasi, M. Cossi, N. Rega, J.M. Millam, M. Klene, J.E. Knox, J.B. Cross, V. Bakken, C. Adamo, J. Jaramillo, R. Gomperts, R.E. Stratmann, O. Yazyev, A.J. Austin, R. Cammi, C. Pomelli, J.W. Ochterski, R.L. Martin, K. Morokuma, V.G. Zakrzewski, G.A. Voth, P. Salvador, J.J. Dannenberg, S. Dapprich, A.D. Daniels, O. Farkas, J.B. Foresman, J.V. Ortiz, J. Cioslowski, and D.J. Fox, Gaussian 09, Gaussian, Inc., Wallingford, CT, 2009.

41. Becke, A.D. Density functional thermochemistry. III. The role of exact exchange. *J. Chem. Phys.* **1993**, *98*, 5648–5652.
42. Adamo, C.; Barone, V.Toward reliable density functional methods without adjustable parameters: the PBE0 model. *J. Chem. Phys.* **1999**, *110*, 6158–6170.
43. Yanai, T.; Tew, D.P.; Handy, N.C. A new hybrid exchange–correlation functional using the coulomb-attenuating method (CAM-B3LYP). *Chem. Phys. Lett.* **2004**, *393*, 51–57.
44. Zhao, Y.; Truhlar, D.G. The M06 suite of density functionals for main group thermochemistry, thermochemical kinetics, noncovalent interactions, excited states, and transition elements: two new functionals and systematic testing of four M06-class functionals and 12 other functionals. *Theor. Chem. Acc.* **2008**, *120*, 215–241.
45. Adamo, C.; Barone, V. Exchange functionals with improved long-range behavior and adiabatic connection methods without adjustable parameters: The mPW and mPW1PW models. *J. Chem. Phys.* **1998**, *108*, 664–675.
46. Chai, J.D.; Head-Gordon, M.. Toward reliable density functional methods without adjustable parameters: The PBE0 model. *Phys. Chem. Chem. Phys.* **2008**, *10*, 6615–6620.
47. R.A. Marcus, Chemical and electrochemical electron-transfer theory, Annu. Rev. Phys. Chem. 15 (1964) 155–196.
48. Marcus, R.A. Electron transfer reactions in chemistry. Theory and experiment, *Rev. Mod. Phys.* **1993**, *65*, 599–610.
49. [49] Köse, M.E.; Mitchell, W.J.; Kopidakis, N.; Chang, C.H.; Shaheen, S.E.; Kim, K.; Rumbles, G. *J. Am. Chem. Soc.* **2007**, *129*, 14257–14270.
50. Pearson, R.G. Absolute electronegativity and absolute hardness of Lewis acids and bases. *J. Am. Chem. Soc.* 1985, 107, 6801–6806.
51. Start, M.S. Epoxidation of alkenes by peroxyl radicals in the gas phase: structure–activity relationships. *J. Phys. Chem. A* **1997**, *101*, 8296–8301.
52. Chaudhry, A.R.; Ahmed, R.; Irfan, A.; Muhammad, S.; Shaari, A.; Al-Sehemi, A.G. Influence of push–pull configuration on the electro-optical and charge transport properties of novel naphtho-difuran derivatives: a DFT study. RSC Adv. 4 (2014) 48876–48887.
53. Irfan, A.; Zhang, J. Effect of one ligand substitution on charge transfer and optical properties in mer-Alq3: A theoretical study. Theor. Chem. Acc. 124 (2009) 339–344.
54. Chaudhry, A.R.; Ahmed, R.; Irfan, A.; Shaari, A.; Al-Sehemi, A.G. Effects of electron withdrawing groups on transfer integrals, mobility, electronic and photo-phys- ical properties of naphtho[2,1-b:6,5-b]difuran derivatives: a theoretical study. Sci. Adv. Mater. 6 (2014) 1727–1739.